



## Removal of nickel from aqueous solution using magnesite tailing

Seda Erol, Mine Özdemir\*

Department of Chemical Engineering, Eskişehir Osmangazi University, 26480 Eskişehir, Turkey, Tel. +90 222 2393750, ext. 3677; Fax: +90 222 2393613; email: [mnozdemir@ogu.edu.tr](mailto:mnozdemir@ogu.edu.tr) (M. Özdemir)

Received 26 March 2014; Accepted 27 December 2014

### ABSTRACT

The removal of nickel ions from aqueous solutions using magnesite tailing was studied in batch system. The effects of initial pH, adsorbent dosage, contact time, and temperature on nickel removal were investigated. Kinetic models were evaluated to describe the kinetics of nickel adsorption onto magnesite tailing. The adsorption kinetics conformed to the pseudo-second-order kinetic model. The Langmuir and Freundlich models were used for the analysis of adsorption equilibrium. The equilibrium data obeyed the Langmuir isotherm model. The thermodynamic parameters exhibited that the adsorption process was spontaneous and endothermic. The Fourier transform infrared spectroscopy analysis was applied to characterize the unloaded and nickel-loaded magnesite tailing. The functional groups such as hydroxyl, carbonate, silicon oxide, and iron oxide on the adsorbent surface may be responsible for nickel adsorption.

*Keywords:* Nickel removal; Adsorption; Magnesite tailing; Isotherm; Kinetics

### 1. Introduction

The existence of heavy metals in aquatic systems can be detrimental to a variety of living species. Among heavy metals, nickel is one of the most widely used ones in the manufacture of stainless steel, super-alloys, metal alloys, dyes, electroplates, porcelain enamels, coins, and batteries. Direct exposure to nickel causes allergy. The inhaled nickel compounds are carcinogenic and metallic nickel is possibly carcinogenic. A general toxicity value of nickel is 130 µg/L. But, this value may not be sufficiently protective of individuals sensitized to nickel. Thus, World Health Organization recommends a drinking water standard of 0.02 mg/L for nickel [1]. The nickel contents in these wastewaters and waters should be removed by a suitable method.

A few methods for removal of heavy metals from water are chemical precipitation, ion exchange, solvent extraction, and reverse osmosis. These methods are usually costly and ineffective for various concentrations. Adsorption is a feasible alternative method for the removal of metals as it has been found to be very effective, economical, and simple. However, the use of this method is restricted by the high cost of adsorbents such as activated carbon and synthetic ion exchangers. So, natural minerals and tailings have received wide attention recently as potential low-cost adsorbents for the removal of heavy metals [2–21].

Magnesite (MgCO<sub>3</sub>) is one of the most important magnesium minerals. It is the basic source for the production of magnesium and magnesium compounds. These products are extensively used in the manufacture of basic refractory bricks, heat-insulating compositions, paper, plastics, rubber, ink, glass, ceramics,

\*Corresponding author.

paints, and pharmaceuticals. The natural magnesite includes some impurities like calcium carbonate, silica, and ferric oxide. Mechanical beneficiation is used to remove part of these impurities. The purity of the remaining mineral after mechanical beneficiation is inadequate for industrial applications where relatively pure mineral is required [22]. In Turkey, these magnesite tailings are currently simply accumulated in the plant areas. These tailings contain 35–39% MgO. Therefore, it is necessary to utilize these tailings including a high amount of magnesite in order to prevent a storage problem as well as an economical loss [23].

Minerals and clays—such as magnesite, calcite, dolomite, sepiolite, kaolinite, montmorillonite, clinoptilolite, and bentonite—and waste minerals and sludge, low-rank coals and bagasse fly ash have been investigated for use as potential adsorbents for the removal of heavy metals from solutions, due to their availability and comparatively lower cost [2–21]. Magnesite, calcite, and dolomite which are known as carbonate minerals are effective for the removal of heavy metals [3,4,6,8–10,21]. The removal of cesium, barium, chromium, and zinc ions by magnesite was reported in the literature for different pH values and initial concentrations [3,4]. However, no information is available in literature for the removal of nickel by magnesite. The aim of this study is to investigate the usability of magnesite tailing for the removal of nickel from aqueous solutions. The effects of different parameters such as pH, contact time, adsorbent dosage, and temperature on the removal of nickel were examined. Kinetic models were tested to investigate the adsorption kinetics. The Langmuir and Freundlich isotherms were used to evaluate the experimental data. Thermodynamic parameters were also calculated. The unloaded and nickel-loaded magnesite tailings were characterized by Fourier transform infrared spectroscopy (FTIR) analysis.

## 2. Materials and methods

### 2.1. Materials

The magnesite tailing was obtained from the KÜMAŞ Plant in Turkey. It was crushed, ground, and sieved through a 200 mesh sieve. A nickel stock solution of 500 mg/L was first prepared by dissolving an accurate quantity of  $\text{NiCl}_2 \cdot 6\text{H}_2\text{O}$  in deionized water. All solutions for adsorption experiments were prepared by appropriate dilutions from the stock solution. The pH values of the solutions were adjusted using diluted NaOH and HCl solutions. The chemicals used during the experiments and analyses were reagent-grade Merck products.

### 2.2. Characterization

The chemical analysis of the magnesite tailing was carried out using X-ray fluorescence analyzer (XRF ARL 8610). The chemical composition of the magnesite tailing is as follows: 37.80% MgO, 11.17%  $\text{SiO}_2$ , 6.25% CaO, 0.77%  $\text{Fe}_2\text{O}_3$ , 0.13%  $\text{Al}_2\text{O}_3$ , 0.05% MnO, 0.01%  $\text{K}_2\text{O}$ , 0.01%  $\text{P}_2\text{O}_5$ , <0.01%  $\text{Na}_2\text{O}$ , <0.01%  $\text{TiO}_2$ , and 43.70% LOI. The X-ray diffractograms of magnesite tailing and nickel-loaded magnesite tailing were obtained using a Philips X'pert Pro diffractometer (XRD) with Cu  $K\alpha$  (Figs. 1 and 2). Both X-ray diffractograms indicated the presence of magnesite ( $\text{MgCO}_3$ ), quartz ( $\text{SiO}_2$ ), and dolomite ( $\text{CaMg}(\text{CO}_3)_2$ ). The specific surface area (BET—Brunauer, Emmett & Teller), pore size distribution (BJH—Barrett, Joyner & Halenda), and total micropore volume (DR—Dubinin–Radushkevich) of magnesite tailing were determined from  $\text{N}_2$  adsorption isotherm with a surface area analyzer (Quantachrome, Autosorb-1 C). The specific surface area and an average pore diameter of magnesite tailing were measured to be 23.12  $\text{m}^2/\text{g}$  and 9.26 nm, respectively. Magnesite tailing has a high surface area when compared to the surface areas of carbonate minerals [9,10]. The presence of micropores (about 50%) and mesopores (about 50%) was determined in the magnesite tailing (Fig. 3). FTIR spectra of unloaded and nickel-loaded adsorbents were recorded using KBr pellets on a Perkin–Elmer spectrum 100 Model infrared spectrophotometer over 400–4,000/ $\text{cm}$ . The pH of the zero point of charge ( $\text{pH}_{\text{zpc}}$ ) was determined by adding 0.1 g of adsorbent to a series of flasks that contained 50 mL of 0.01 M NaCl. Before adding the adsorbent, the pH of the solution was to be in the range of 2–12 by adding 0.1 M HCl or 0.1 M NaOH. These flasks were kept for 48 h in shaker and the final pH values of the solutions were measured. The  $\text{pH}_{\text{final}}$  values were plotted against the  $\text{pH}_{\text{initial}}$  values. The pH is the point at which the  $\text{pH}_{\text{final}}$  vs.  $\text{pH}_{\text{initial}}$  curve intersects the  $\text{pH}_{\text{initial}} = \text{pH}_{\text{final}}$  line [24]. The  $\text{pH}_{\text{zpc}}$  value of the magnesite tailing was obtained as 8.0. The pH values of the solutions were measured by a pH meter (Hanna HI 8314). The concentrations of the nickel ions were determined by an atomic absorption spectrometer (THERMO ICE 3300).

### 2.3. Adsorption experiments

The adsorption experiments were carried out in 100 mL capped volumetric flasks placed on a temperature-controlled water bath (Nüve) with the shaker (Memmert). A fixed amount of adsorbent was equilibrated to 50 mL of the nickel chloride solution. The adsorbent was removed by centrifugation. The

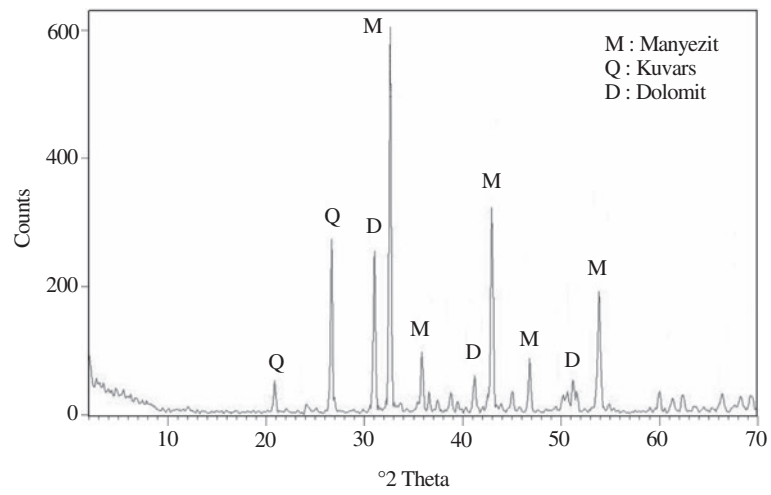


Fig. 1. X-ray diffractogram of magnesite tailing.

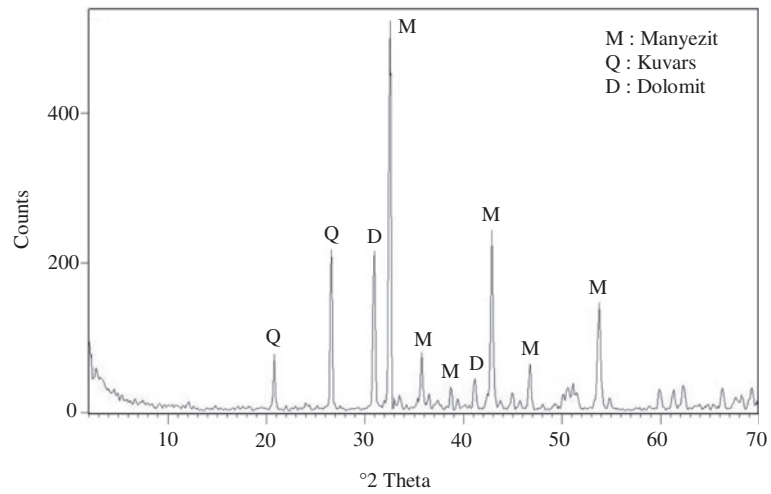


Fig. 2. X-ray diffractogram of nickel-loaded magnesite tailing.

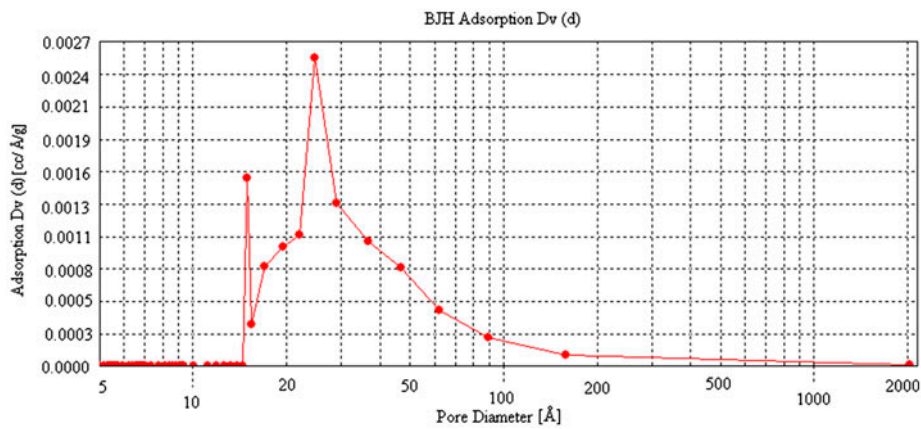


Fig. 3. Pore size distribution of magnesite tailing.

concentration of the nickel remaining in the supernatant was measured by an atomic absorption spectrometer. The amount of nickel adsorbed ( $q_e$ ) and the removal yield were calculated using the following equations, respectively:

$$q_e = \frac{(C_0 - C_e)V}{1,000m} \quad (1)$$

$$\% \text{Removal yield} = \frac{(C_0 - C_e)}{C_0} \times 100 \quad (2)$$

where  $C_0$  is the initial concentration of nickel (mg/L),  $C_e$  is the concentration of nickel at equilibrium (mg/L),  $V$  is the volume of solution (mL), and  $m$  is the mass of magnesite tailing (g).

To examine the effect of pH, the experiments were performed at varied pH values (2–8) under the conditions of adsorbent dosage of 0.01 g/50 mL, contact time of 24 h, temperature of 25°C, and initial nickel concentration of 10 mg/L.

The adsorption of 10 mg/L of nickel chloride solution by different adsorbent dosages (0.01–0.2 g/50 mL) was carried out at a pH value of 6.0, a contact time of 24 h, and a temperature of 25°C.

Batch experiments were also repeated for various time intervals to determine when the adsorption equilibrium was reached at the constant conditions of pH value of 6.0, adsorbent dosage of 0.15 g/50 mL, and initial nickel concentration of 10 mg/L for temperatures of 25, 35, and 45°C.

Nickel adsorption experiments were accomplished to obtain the isotherms for a range of 10–50 mg/L at a pH value of 6.0, an adsorbent dosage of 0.15 g/50 mL, a contact time of 24 h, and at various temperatures (25–45°C).

The average absolute value of relative error (AARE) is used to compare the predicted results with the experimental data. This is defined as follows:

$$\text{AARE} = \frac{1}{N} \sum_{i=1}^N \left( \frac{|\text{Predicted value} - \text{Experimental value}|}{\text{Experimental value}} \right) \quad (3)$$

### 3. Results and discussion

#### 3.1. Effect of initial pH

The effect of initial pH on the adsorption of nickel was examined in the pH range of 2–8. When pH increased from 2 to 8, the removal yield increased (Fig. 4). The maximum removal yield was obtained at pH values higher than 6. The effect of pH can be explained in terms of  $\text{pH}_{\text{zpc}}$  of the adsorbent and

species of nickel formed in the solution. The pH value with which the charge of the solid surface is zero is defined as the zero point of charge ( $\text{pH}_{\text{zpc}} = 8.0$ ). At low  $\text{pH}_{\text{zpc}}$  the surface charge of the adsorbent is positive while it is negative above  $\text{pH}_{\text{zpc}}$ . At pH values lower than 8,  $\text{Ni}^{2+}$  and  $\text{Ni}(\text{OH})^+$  are dominant species [12,25]. At  $\text{pH} > 6$ , the positive surface charge of the adsorbent decreased and the number of negatively charged sites increased, and, thus, the adsorbent surface attracted more positively charged adsorbate particles,  $\text{Ni}^{2+}$  and  $\text{Ni}(\text{OH})^+$ . The lowest nickel removal was obtained at pH 2. At  $\text{pH} < 6$ , the increased number of protons on the sites of magnesite tailing surface limited the approach of  $\text{Ni}^{2+}$  due to the repulsive forces. These results are in agreement with those of the previous studies [15,16,20].

#### 3.2. Effect of adsorbent dosage

The effect of adsorbent dosage on nickel removal is shown in Fig. 5 for a 50 mL portion of the 10 mg/L nickel solution. When the adsorbent dosage increased from 0.01 to 0.15 g, the nickel removal yield increased from 14.19 to 84.45%. This increase may be attributed to the increase in the adsorbent surface area of magnesite tailing and/or adsorptive sites. A further increase in adsorbent dosage over 0.15 g did not lead to a significant change in the nickel removal. This situation may be related to a decrease in the nickel concentration of the solution. Therefore, the optimum adsorbent dosage was taken as 0.15 g.

#### 3.3. Effect of contact time and temperature

The effect of contact time on the adsorption of nickel at three different temperatures is presented in

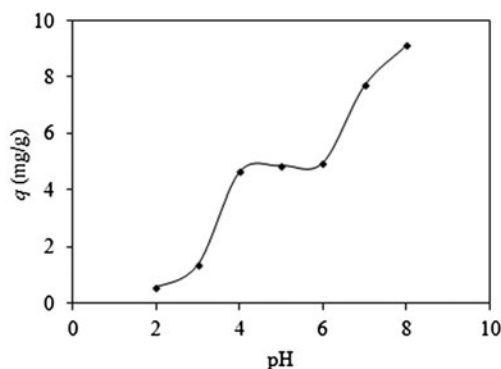


Fig. 4. Effect of initial pH on the adsorption of nickel by magnesite tailing (adsorbent dosage = 0.01 g/50 mL, contact time = 24 h, temperature = 25°C, and initial nickel concentration = 10 mg/L).

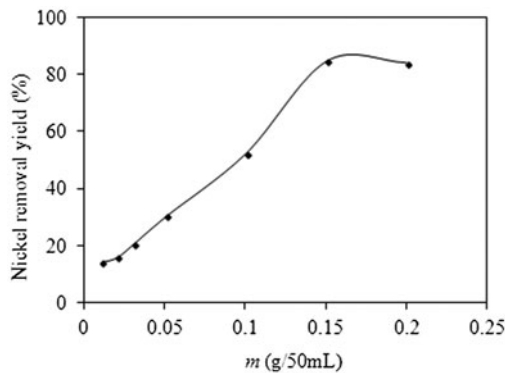


Fig. 5. Effect of adsorbent dosage on the adsorption of nickel by magnesite tailing (pH 6.0, contact time = 24 h, temperature = 25°C, and initial nickel concentration = 10 mg/L).

Fig. 6. The adsorption rate was initially fast and 50% adsorption was completed within 120, 5, and 5 min for 25, 35, and 45°C, respectively. The adsorption equilibrium was achieved within about 720 min. Furthermore, as shown in Fig. 6, the adsorption capacity of magnesite tailing increased with an increase in the temperature from 25 to 45°C. This situation revealed that the adsorption process was endothermic.

### 3.4. Adsorption kinetics

In order to describe the kinetics of nickel adsorption onto magnesite tailing, the obtained kinetic data were analyzed using three kinetic models: pseudo-first-order, pseudo-second-order kinetic equations and intraparticle diffusion models. The pseudo-first-order equation presented by Lagergren [26], can be given as follows:

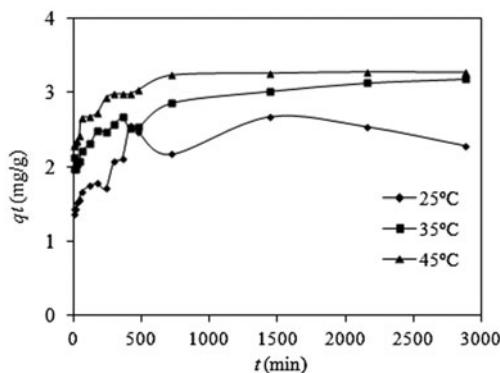


Fig. 6. Effect of contact time on the adsorption of nickel by magnesite tailing at different temperatures (pH 6.0, adsorbent dosage = 0.15 g/50 mL, and initial nickel concentration = 10 mg/L).

$$\log(q_e - q_t) = \log q_e - \frac{k_1 t}{2.303} \quad (4)$$

where  $q_e$  and  $q_t$  are the respective amounts of nickel adsorbed (mg/g) at equilibrium and at time  $t$  (min) and  $k_1$  (1/min) is the rate constant of the pseudo-first-order adsorption.

The pseudo-second-order equation described by Ho and McKay [27] may be expressed in the form:

$$\frac{t}{q_t} = \frac{1}{k_2 q_e^2} + \frac{t}{q_e} \quad (5)$$

where  $k_2$  (g/mg min) is the rate constant of pseudo-second-order adsorption.

If there is the possibility of intraparticle diffusion being the rate-limiting step, the intraparticle diffusion rate constant can be obtained from Eq. (6) based on the theory proposed by Weber and Morris [28]:

$$q_t = k_p t^{1/2} + C \quad (6)$$

where  $k_p$  (mg/g min<sup>1/2</sup>) is the intraparticle diffusion rate constant (slope of the plot of  $q_t$  vs.  $t^{1/2}$ ) and  $C$  is the constant related to the boundary layer thickness.

The plots of  $\log(q_e - q_t)$  vs.  $t$ ,  $t/q_t$  vs.  $t$ , and  $q_t$  vs.  $t^{1/2}$  obtained from these models were checked statistically and graphically (Fig. 7 for  $t/q_t$  vs.  $t$ ). The kinetic parameters of these models were calculated using linear least-squares fittings (Table 1). The correlation coefficients of pseudo-first-order kinetic model were found to be lower, and the calculated  $q_e$  values also gave different values compared to the experimental values. The correlation coefficients of intraparticle diffusion model were also lower, and the plots of  $q_t$  vs.  $t^{1/2}$  did not pass through the origin. These results showed that intraparticle diffusion was not the rate-limiting mechanism. The correlation coefficients of pseudo-second-order kinetic model were higher and the calculated  $q_e$  values showed greater agreement with the experimental data with an average deviation of 0.79%. The pseudo-second-order kinetic model indicates that the chemisorption would be the rate-determining step controlling the adsorption process of nickel ion.

### 3.5. Adsorption isotherms

Adsorption isotherm can be indicated graphically by plotting the amount of adsorbed nickel per unit amount of magnesite tailing against equilibrium concentration of nickel (Fig. 8). The isotherm is an L2 type, indicating that the adsorbate-adsorbent interaction is

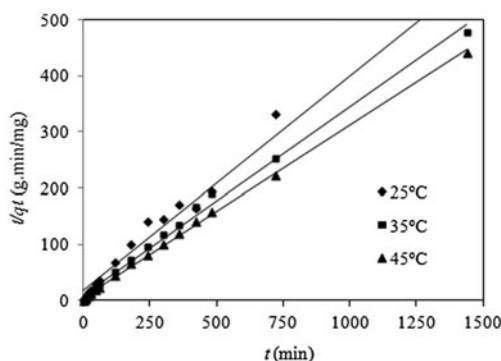


Fig. 7. Pseudo-second-order kinetic plots for the adsorption of nickel onto magnesite tailing at different temperatures.

much stronger than the solvent–adsorbent interaction at the adsorption sites [29]. The adsorption capacity of the magnesite tailing increased with initial concentration and temperature. When the initial nickel solution concentration increased from 10 to 50 mg/L, the adsorption capacities increased from 2.28 to 3.78 mg/g at 25°C and from 3.34 to 5.37 mg/g at 45°C.

The relationship between the adsorbed amount of nickel and its equilibrium concentration in the solution was described by the Langmuir and Freundlich isotherms, which are the most common isotherm equations. These isotherms are expressed by the following equations, respectively [30].

$$q_e = \frac{q_0 b C_e}{1 + b C_e} \quad (7)$$

$$q_e = K_f C_e^{1/n} \quad (8)$$

These equations can be rearranged to linear forms:

$$\frac{C_e}{q_e} = \frac{1}{q_0 b} + \frac{C_e}{q_0} \quad (9)$$

$$\log q_e = \log K_f + \left(\frac{1}{n}\right) \log C_e \quad (10)$$

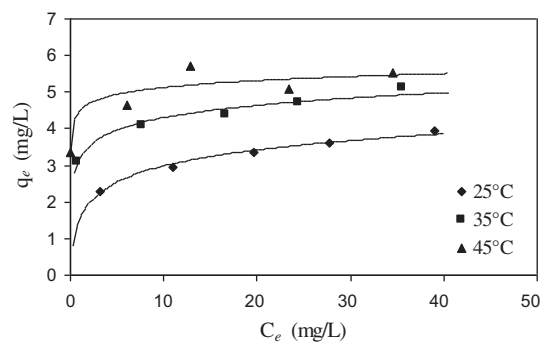


Fig. 8. Isotherms for the adsorption of nickel onto magnesite tailing at different temperatures.

where  $q_e$  is the adsorbed amount per amount of adsorbent at equilibrium (mg/g),  $C_e$  is the equilibrium concentration in the solution (mg/L), and the Langmuir constants  $q_0$  (mg/g) and  $b$  (L/mg) are the monolayer adsorption capacity and the adsorption equilibrium constant, respectively.  $K_f$  (L/g) and  $n$  are Freundlich adsorption isotherm constants related to the adsorption capacity and the adsorption intensity, respectively. The comparison of the experimental values with the values of  $q_e$  obtained by the models of Langmuir and Freundlich at different temperatures are shown in Fig. 9. The Langmuir isotherm usually fitted better with the experimental data. The isotherm constants, linear correlation coefficients, and AARE values at different temperatures are presented in Table 2. The correlation coefficients are usually higher in the Langmuir isotherm. The Langmuir isotherm is specific for monolayer adsorption. The Langmuir equilibrium coefficient  $b$  determines the direction of the adsorbate–adsorbent equilibrium. The values of  $b$  increased with an increase in the temperature. Higher values showed that the equilibrium moved to the formation of the adsorbate–adsorbent complex.

The separation factor ( $R_L$ ) can be used to confirm the favorability of the adsorption process [31]. The  $R_L$  value is calculated using the following equation:

Table 1  
Kinetic parameters for the adsorption of nickel by magnesite tailing at different temperatures

$T$ (°C)	$q_{exp}$ (mg/g)	Pseudo-first-order			Pseudo-second-order			Intraparticle diffusion		
		$q_e$ (mg/g)	$k_1$ (1/min)	$R^2$	$q_e$ (mg/g)	$k_2$ (g/mg min)	$R^2$	$k_p$ (mg/g min <sup>1/2</sup> )	$C$ (mg/g)	$R^2$
25	2.67	1.20	0.003	0.54	2.64	0.008	0.98	0.040	1.32	0.85
35	3.02	0.98	0.002	0.89	3.00	0.010	0.99	0.031	1.95	0.93
45	3.26	1.04	0.004	0.92	3.28	0.015	0.99	0.033	2.28	0.89

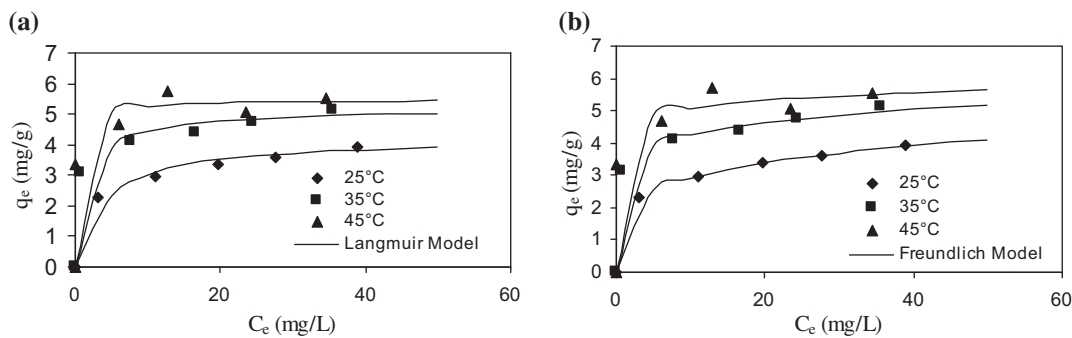


Fig. 9. Comparison of the experimental values with the  $q_e$  values obtained by Langmuir (a) and Freundlich (b) isotherms.

$$R_L = \frac{1}{1 + bC_0} \quad (11)$$

where  $C_0$  is the initial nickel concentration (mg/L). If  $R_L > 1$ , the isotherm is unfavorable; if  $R_L = 1$ , the isotherm is linear; if  $0 < R_L < 1$ , the isotherm is favorable; and if  $R_L = 0$ , the isotherm is irreversible [31,32]. The values of  $R_L$  calculated from Eq. (11) are in Table 2. The  $R_L$  values for the adsorption of nickel are between 0.01 and 0.28, and so its adsorption is favorable. The maximum adsorption capacities were found to be 4.22 mg/g at 25°C, 5.21 mg/g at 35°C, and 5.48 mg/g at 45°C.

The adsorption capacities found in the present study were compared with those of other adsorbents used in previous studies (Table 3). It was seen that the adsorption capacity of the magnesite tailing was higher than those of kaolinite, clinoptilolite, calcined Bofe bentonite clay, dolomite, iron oxide, and manganese oxide-coated sand [5,17,20,21,33]. In addition, it can be obtained cheaply in large amounts.

### 3.6. Thermodynamic parameters

Thermodynamic parameters were studied to reveal the nature of the adsorption process. The thermodynamic parameters such as the changes in free energy ( $\Delta G^\circ$ ), enthalpy ( $\Delta H^\circ$ ), and entropy ( $\Delta S^\circ$ ) can be

calculated using the Langmuir equilibrium constants (b) which change with temperature. These parameters are found by using the following equations:

$$\Delta G^\circ = -RT \ln b \quad (12)$$

$$\ln b = \frac{\Delta S^\circ}{R} - \frac{\Delta H^\circ}{RT} \quad (13)$$

where  $R$  is the gas constant (8.314 J/mol K) and  $T$  is the solution temperature (K). The values of  $\Delta H^\circ$  and  $\Delta S^\circ$  were calculated from the slopes and intercepts of the linear regression of  $\ln b$  vs.  $1/T$  (Fig. 10). The calculated parameters are given in Table 4. The positive value of  $\Delta H^\circ$  (87.98 kJ/mol) exhibits that the adsorption is endothermic. Furthermore, the positive value and magnitude of  $\Delta H^\circ$  imply that the nature of the adsorption is a chemical process involving sharing or transfer of electrons between adsorbent and adsorbate. The negative values of  $\Delta G^\circ$  (−23.51, −27.25, and −30.99 kJ/mol) indicate that the adsorption of nickel on the magnesite tailing is spontaneous for the studied temperature range. The change of free energy for the exchange process is between −8 and −16 kJ/mol [34]. The  $\Delta G^\circ$  values up to −20 kJ/mol indicate physical adsorption while  $\Delta G^\circ$  values more negative than −40 kJ/mol involve chemical adsorption [35]. Thus, the nickel adsorption by magnesite tailing may be

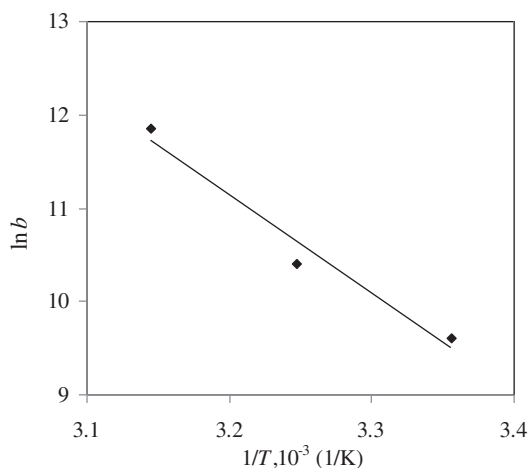
Table 2  
Langmuir and Freundlich constants for nickel adsorption by magnesite tailing at different temperatures

Temperature (°C)	Langmuir				Freundlich				
	$q_0$ (mg/g)	$b$ (L/mg)	$R^2$	AARE%	$R_L$	$K_f$ (L/g)	$n$	$R^2$	AARE%
25	4.22	0.253	0.993	3.36	0.28–0.07	1.798	4.74	0.999	2.96
35	5.21	0.564	0.993	0.16	0.15–0.03	3.187	8.05	0.986	0.79
45	5.48	2.375	0.994	0.44	0.04–0.01	4.387	15.67	0.908	0.86

Table 3

Comparisons of the Langmuir adsorption capacities ( $q_0$ ) for nickel adsorption by different adsorbents

Type of adsorbent	$q_0$ (mg/g)	$b$ (L/mg)	Temp. (°C)	pH	Refs.
Kaolinite	1.67	0.112	25		[5]
	2.79	0.240	40		
Sewage sludge ash	7.65	0.051	20	6.0	[7]
Bagasse fly ash	6.49	0.153	306.0	6.0	[12]
Low-rank coal	7.63	0.188	22	4.0	[13]
Kaolinite	7.1	0.057	30	5.7	[15]
Acid-activated kaolinite	9.9	0.070	30	5.7	[16]
Montmorillonite	21.1	0.138	30	5.7	[15]
Acid-activated montmorillonite with tartaric acid	21.3	0.238	30	5.7	[16]
Clinoptilolite	3.28	0.182	20	7.0	[17]
Calcined Bofe bentonite clay	2.88	0.071	20	5.3	[20]
	3.89	0.056	75	5.3	
Dolomite	5.41	0.011	20	5.5	[21]
Iron oxide coated sand	2.93	0.20	20		[33]
Manganese oxide coated sand	3.33	0.34	20		[33]
Magnesite tailing	4.22	0.293	25	6.0	Present study
	5.48	4.011	45	6.0	Present study

Fig. 10. Plot of  $\ln b$  vs.  $1/T$  for estimation of thermodynamic parameters.

physical adsorption or chemical adsorption. However, the degree of spontaneity increases with temperature. This is because the adsorption process contains mainly chemical adsorption rather than physical adsorption.

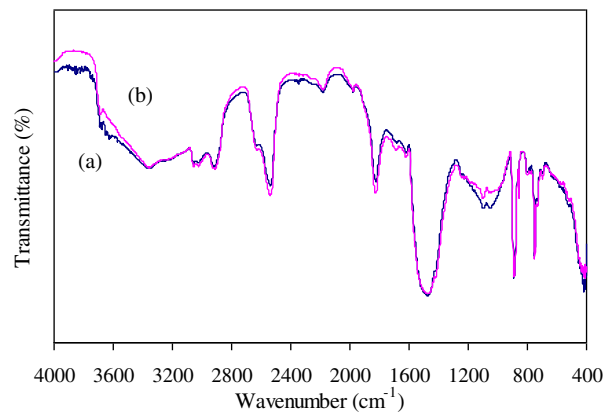


Fig. 11. FTIR spectra of unloaded (a) and nickel-loaded (b) magnesite tailing.

The positive value of  $\Delta S^\circ$  (0.374 kJ/mol K) indicates an increase in the randomness at the solid–solution interface and reflects the affinity of magnesite tailing toward nickel ions. Similar findings were reported for some other natural adsorbents [5,10,14,19,33].

Table 4

Thermodynamic parameters for the adsorption of nickel by magnesite tailing

Temperature (°C)	$\Delta G^\circ$ (kJ/mol)	$\Delta H^\circ$ (kJ/mol)	$\Delta S^\circ$ (kJ/mol K)
25	-23.51	87.98	0.374
35	-27.25		
45	-30.99		

Table 5  
Functional groups in unloaded and nickel-loaded adsorbents

Functional group	Wavenumber (cm <sup>-1</sup> )	
	Unloaded adsorbent	Nickel-loaded adsorbent
Surface hydroxyl groups (Si–OH–Si)	3,690–3,678–3,650–3,630–3,615	3,688
–OH stretching	3,358–3,050–3,020–2,915	3,355–3,055–3,023–2,913
–CO <sub>3</sub> <sup>2-</sup> stretching-bending	2,535	2,535
–CO <sub>3</sub> <sup>2-</sup> stretching	1,825	1,825
–OH bending	1,685–1,618	1,688–1,623
–CO <sub>3</sub> <sup>2-</sup> asymmetric stretching	1,473–1,418	1,473–1,418
–CO <sub>3</sub> <sup>2-</sup> symmetric stretching	1,095–1,058	1,100–1,060
–CO <sub>3</sub> <sup>2-</sup> out of plane bending	890–858	890–858
Si–O stretching vibration	798–780	800–780
–CO <sub>3</sub> <sup>2-</sup> in plane bending	750	750
Mg–OH bending vibration	695	698
Si–O or Fe–O bending vibrations	420–410	430–423–408

### 3.7. FTIR analysis

The FTIR spectra of the magnesite tailing and nickel-loaded magnesite tailing are shown in Fig. 11. The possible functional groups for each sample are presented in Table 5. The FTIR spectra show that the magnesite tailing are mainly composed of carbonate, silicon oxide, iron oxide, and hydroxyl groups (Fig. 11(a)) [9,36]. In the FTIR spectrum of unloaded adsorbent, the bands ranging from 2,915 to 3,690/cm were related to the –OH stretching vibration. The absorption bands at 2,535–1,825, 1,473–1,418, and 1,095–1,058/cm showed the characteristic stretching of –CO<sub>3</sub> group. The weak bands observed at 1,685 and 1,618/cm were assigned to the –OH bending. The sharp absorption bands at 890–858–750 showed the characteristic bending of –CO<sub>3</sub> group. The very weak band observed at 695/cm was produced by Mg–OH bending vibration. The absorption bands appearing at 420 and at 410/cm indicated the existence of –Si–O or –Fe–O bending vibrations (Fig. 11(a)). These groups are likely to be responsible for nickel adsorption. Some peaks indicating surface hydroxyl groups disappeared in the FTIR spectrum of the nickel-loaded magnesite tailing (Fig. 11(b)). The shifts in the wave numbers of the –OH stretching, –OH bending, –CO<sub>3</sub><sup>2-</sup> symmetric stretching, Si–O stretching vibration, and Mg–OH bending vibration were observed. The peaks of –Si–O or –Fe–O bending vibrations at 420 and 410/cm were separated into 430, 423, and 408/cm peaks. The FTIR spectra showed the hydroxyl, carbonate, silicon oxide, and iron oxide groups that were included in the adsorption process.

### 4. Conclusions

In this study, the removal of nickel from aqueous solution was investigated using magnesite tailing. The optimum pH was found as 6.0. The adsorption equilibrium was nearly attained at 720 min. The kinetic data were better represented by a pseudo-second-order kinetic model. The adsorption process followed the Langmuir isotherm model. The maximum Langmuir adsorption capacity was determined to be 5.48 mg/g at 45°C. The thermodynamic studies showed the spontaneous, endothermic, and random nature of the process. The nickel–magnesite tailing interactions were confirmed by FTIR analysis. The hydroxyl, carbonate, silicon oxide, and iron oxide groups on the adsorbent surface were found to be responsible for nickel adsorption. The magnesite tailing may be used for the removal of nickel from wastewater, since it is a low cost and locally available adsorbent.

### List of symbols

$b$	—	adsorption equilibrium constant (L/mg)
$C$	—	constant related to the boundary layer thickness
$C_e$	—	concentration of nickel at equilibrium (mg/L)
$C_0$	—	initial concentration of nickel (mg/L)
$k_1$	—	rate constant of the pseudo-first-order adsorption (1/min)
$k_2$	—	rate constant of pseudo-second-order adsorption (g/mg min)
$k_p$	—	intraparticle diffusion rate constant (mg/g min <sup>1/2</sup> )
$K_{a1}$	—	hydrolysis constant
$K_f$	—	Freundlich adsorption isotherm constant related to the adsorption capacity (L/g)
$m$	—	mass of magnesite tailing (g)

- $n$  — Freundlich adsorption isotherm constant related to the adsorption intensity
- $q_0$  — monolayer adsorption capacity (mg/g)
- $q_e$  — adsorption capacity at equilibrium (mg/g)
- $q_t$  — adsorption capacity at time  $t$  (mg/g)
- $R$  — universal gas constant (8.314 J/mol K)
- $R_L$  — separation factor
- $t$  — time (min)
- $T$  — solution temperature (K)
- $V$  — volume of solution (mL)
- $\Delta G^\circ$  — Gibb's free energy change (kJ/mol)
- $\Delta H^\circ$  — enthalpy change (kJ/mol)
- $\Delta S^\circ$  — entropy change (kJ/mol K)

### Acknowledgments

This study was financially supported by Eskişehir Osmangazi University Research Foundation (Project No. 200815036). We also thank Dr Hakan Demiral and Dr Ceyda Bilgiç for BET and FTIR measurements, respectively.

### References

- [1] WHO, Guidelines for Drinking Water Quality, fourth ed., WHO, Geneva, 2011.
- [2] S.E. Bailey, T.J. Olin, R.M. Bricka, D.D. Adrian, A review of potentially low-cost sorbents for heavy metals, *Water Res.* 33 (1999) 2469–2479.
- [3] T. Shahwan, S. Suzer, H.N. Erten, Sorption studies of  $\text{Cs}^+$  and  $\text{Ba}^{2+}$  cations on magnesite, *Appl. Radiat. Isot.* 49 (1998) 915–921.
- [4] M. Lehmann, A.L. Zouboulis, K.A. Matis, Removal of metal ions from dilute aqueous solutions: A comparative study of inorganic sorbent materials, *Chemosphere* 39 (1999) 881–892.
- [5] Ö. Yavuz, Y. Altunkaynak, F. Güzel, Removal of copper, nickel, cobalt and manganese from aqueous solution by kaolinite, *Water Res.* 37 (2003) 948–952.
- [6] G.M. Walker, J.A. Hanna, S.J. Allen, Treatment of hazardous shipyard wastewater using dolomitic sorbents, *Water Res.* 39 (2005) 2422–2428.
- [7] Z. Elouear, J. Bouzid, N. Boujelben, Removal of nickel and cadmium from solutions by sewage sludge ash: Study in single and binary systems, *Environ. Technol.* 30 (2009) 561–570.
- [8] S. Lee, J.A. Dyer, D.L. Sparks, N.C. Scrivner, E.J. Elzinga, A multi-scale assessment of Pb(II) sorption on dolomite, *J. Colloid Interface Sci.* 298 (2006) 20–30.
- [9] Y.S. Al-Degs, M.I. El-Barghouthi, A.A. Issa, M.A. Khraisheh, G.M. Walker, Sorption of Zn(II), Pb(II), and Co(II) using natural sorbents: Equilibrium and kinetic studies, *Water Res.* 40 (2006) 2645–2658.
- [10] N. Dali-youcef, B. Ouddane, Z. Derriche, Adsorption of zinc on natural sediment of Tafna River (Algeria), *J. Hazard. Mater.* 137 (2006) 1263–1270.
- [11] M.F. Brigatti, C. Lugli, L. Poppi, Kinetics of heavy-metal removal on recovery in sepiolite, *Appl. Clay Sci.* 16 (2006) 45–57.
- [12] V.C. Srivastava, I.D. Mall, I.M. Mishra, Equilibrium modelling of single and binary adsorption of cadmium and nickel onto bagasse fly ash, *Chem. Eng. J.* 117 (2006) 79–91.
- [13] P. Janoš, J. Sypecká, P. Mlčkovská, P. Kuráň, V. Pilařová, Removal of metal ions from aqueous solutions by sorption onto untreated low-rank coal (oxihumolite), *Sep. Purif. Technol.* 53 (2007) 322–329.
- [14] C.H. Weng, C.Z. Tsai, S.H. Chu, Y.C. Sharma, Adsorption characteristics of copper (II) onto spent activated clay, *Sep. Purif. Technol.* 54 (2007) 187–197.
- [15] S.S. Gupta, K.G. Bhattacharyya, Immobilization of Pb(II), Cd(II) and Ni(II) ions on kaolinite and montmorillonite surfaces from aqueous medium, *J. Environ. Manage.* 87 (2008) 46–58.
- [16] K.G. Bhattacharyya, S.S. Gupta, Influence of acid activation on Ni(II) and Cu(II) on kaolinite and montmorillonite: Kinetic and thermodynamic study, *Chem. Eng. J.* 136 (2008) 1–13.
- [17] M.E. Argun, Use of clinoptilolite for the removal of nickel ions from water: Kinetics and thermodynamics, *J. Hazard. Mater.* 150 (2008) 587–595.
- [18] P.C. Mishra, R.K. Patel, Removal of lead and zinc ions from water by low cost adsorbents, *J. Hazard. Mater.* 168 (2009) 319–325.
- [19] N. Rajic, D. Stajkovic, M. Jovanic, N.Z. Logar, M. Mazaj, V. Kaucic, Removal of nickel (II) ions from aqueous solutions using the natural clinoptilolite and preparation of nano-NiO on the exhausted clinoptilolite, *Appl. Surf. Sci.* 257 (2010) 1524–1532.
- [20] M.G.A. Vieira, A.F. Almeida Neto, M.L. Gimenes, M.G.C. da Silva, Sorption kinetics and equilibrium for the removal of nickel ions from aqueous phase on calcined Bofe bentonite clay, *J. Hazard. Mater.* 177 (2010) 362–371.
- [21] M. Mohammadi, A. Ghaemi, M. Torab-Mostaedi, M. Asadollahzadeh, A. Hemmati, Adsorption of cadmium (II) and nickel (II) on dolomite powder, *Desalin. Water Treat.* (2013) 1–9.
- [22] K. Othmer, *Encyclopedia of Chemical Technology*, second ed., Wiley, New York, NY, 1978.
- [23] M. Özdemir, D. Çakır, İ. Kıpçak, Magnesium recovery from magnesite tailings by acid leaching and production of magnesium chloride hexahydrate from leaching solution by evaporation, *Int. J. Miner. Process* 93 (2009) 209–212.
- [24] V.K. Gupta, A. Nayak, Cadmium removal and recovery from aqueous solutions by novel adsorbents prepared from orange peel and  $\text{Fe}_2\text{O}_3$  nanoparticles, *Chem. Eng. J.* 180 (2012) 81–90.
- [25] N.V. Plyasunova, Y. Zhang, M. Muhammed, Critical evaluation of thermodynamics of complex formation of metal ions in aqueous solutions. IV. Hydrolysis and hydroxo-complexes of  $\text{Ni}^{2+}$  at 298.15 K, *Hydrometallurgy* 48 (1998) 43–63.
- [26] S. Lagergren, Zur theorie der sogenannten adsorption gelöster stoffe (To the theory of the so-called adsorption of dissolved substances), *Kungliga Svenska Vetenskapsakademiens Handlingar* 24 (1898) 1–39.
- [27] Y.S. Ho, G. McKay, Sorption of dye from aqueous solution by peat, *Chem. Eng. J.* 70 (1998) 115–124.

- [28] W.J. Weber, J.C. Morris, Kinetics of adsorption on carbon from solution, *J. Sanitary Eng. Div. ASCE*. 89 (1963) 31–59.
- [29] C.H. Giles, T.H. MacEwan, S.N. Nakhwa, D. Smith, Studies in adsorption: Part XI. A system of classification of solution adsorption isotherms, and its use in diagnosis of adsorption mechanisms and in measurement of specific surface areas of solids, *J. Chem. Soc.* 786 (1960) 3973–3993.
- [30] R.E. Treybal, *Mass-Transfer Operations*, third ed., McGraw-Hill, New York, NY, 1981.
- [31] K.R. Hall, L.C. Eagleton, A. Acrivos, T. Vermeulen, Pore- and solid-diffusion kinetics in fixed-bed adsorption under constant-pattern conditions, *Ind. Eng. Chem. Fundam.* 5 (1966) 212–223.
- [32] T.W. Weber, R.K. Chakravorti, Pore and solid diffusion models for fixed bed adsorbers, *J. Am. Inst. Chem. Eng.* 20 (1974) 228–238.
- [33] N. Boujelben, J. Bouzid, Z. Elouear, Retention of nickel from aqueous solutions using iron oxide and manganese oxide coated sand: kinetic and thermodynamic studies, *Environ. Technol.* 31 (2010) 1623–1634.
- [34] F. Helfferich, *Ion-Exchange*, McGraw-Hill, New York, NY, 1964.
- [35] C.H. Weng, C.Z. Tasai, S.H. Chu, Y.C. Sharma, Adsorption characteristics of copper (II) onto spent activated clay, *Sep. Purif. Technol.* 54 (2007) 187–197.
- [36] R.L. Frost, S. Bahfenne, Raman and mid-IR spectroscopic study of the magnesium carbonate minerals-brugnatellite and coalingite, *J. Raman Spectrosc.* 40 (2009) 360–365.